JOURNAL OF MATERIALS SCIENCE 18 (1983) 1958–1966

Mechanical properties and fracture behaviour of ZrO_2–Y_2O_3 ceramics

A. J. A. WINNUBST, K. KEIZER, A. J. BURGGRAAF
Twente University of Technology, Department of Chemical Engineering, Laboratory of Inorganic Chemistry and Materials Science, PO Box 217, 7500 AE Enschede, The Netherlands

Stabilized ZrO_2–Y_2O_3 ceramics have been prepared with varying grain sizes and microstructures with the help of different preparation techniques. Bi_2O_3 has been added as a sinter aid to some of the samples. This results in a certain amount of a zirconia-rich second phase. For Bi_2O_3-free samples the fracture toughness (K_{Ic}), and therefore the fracture energy, increases with decreasing grain size. A linear relation with the inverse square root of the average grain size is found. The highest value of K_{Ic} amounts to 4.1 MPa $m^{1/2}$. Fracture toughness values of 1.9 ± 0.2 MPa $m^{1/2}$ are measured for Bi_2O_3 containing materials. The fracture surfaces are intergrannular for Bi_2O_3-containing and transgranular for Bi_2O_3-free samples, respectively.

1. Introduction

Yttria-stabilized zirconia ceramics exhibit a high oxygen ion conduction at elevated temperatures. These materials are suitable for use in batteries, fuel cells, oxygen probes and sensors. In the processing and use of these materials some problems are encountered. Firstly sintering of pure stabilized zirconias is difficult because excessive grain growth occurs at temperatures of 1900 to 2000 K. This grain growth interferes with the densification process and results in porous coarse-grained materials which are not suited for the fabrication of thin-walled objects or layers. Secondly the fracture energy and especially the fracture toughness values (K_{Ic}) are relatively low. K_{Ic}-values of 1.1 MPa $m^{1/2}$ are reported for coarse-grained partially-stabilized zirconia [1] and of 1.5 MPa $m^{1/2}$ for fully-stabilized yttria–zirconia ceramics [2].

The first problem can be solved by using grain growth inhibitors such as SiO_2, Al_2O_3 or TiO_2 [3–5] or by using very effective sintering-promotors such as Bi_2O_3 [2, 6]. Another possibility is to use very fine grained powders (5 to 10 nm) obtained by hydrolysis of zirconium and yttrium alkoxides [7, 8]. With these powders it is possible to prepare dense, stabilized zirconia ceramics at temperatures of 1450 to 1600 K with grain sizes of 0.3 to 1.0 μm, respectively, and porosities smaller than 5% [8–10].

An increase of the fracture energy and the fracture toughness is possible by the use of a stress-induced phase transformation as reported by Gupta *et al.* [1] and Garvie *et al.* [11]. In that case a partially-stabilized zirconia (PSZ) is used with a very small ceramic grain size ($< 0.3\,\mu$m) and a tetragonal structure. Because of this small grain size the tetragonal–monoclinic phase transition is suppressed down to temperatures below room temperature and the structure of the material remains tetragonal. During crack extension a part of the stress energy around the crack-tip is absorbed by a tetragonal/monoclinic phase transition and the fracture toughness, K_{Ic}, increases from values of 1 to 2 MPa $m^{1/2}$ to values of 6 to 10 MPa $m^{1/2}$. In our case this mechanism cannot be used because the oxygen ion conduction of PSZ probably is too low. Recently electrical conductivities of tetragonal zirconia has been reported [12] indicating conductivity values which are not much lower than that of cubic stabilized materials.

Claussen *et al.* [13, 14] increased the fracture toughness by introducing a monoclinic ZrO_2 phase in Al_2O_3 with Si_3N_4 ceramics. The K_{Ic}

0022–2461/83 $03.00 + .12
© *1983 Chapman and Hall Ltd.*

increased by about a factor 2 when 15 vol% ZrO_2 with a grain size of about 1 μm is introduced into the ceramic matrix. In this case the zirconia particles exhibit the normal tetragonal/monoclinic transition during cooling down the ceramic materials. This results in stresses around the zirconia particles. The transformed particles will initiate microcracks in the field of a penetrating macrocrack due to superposition of the transition-induced stresses and the tensile ahead of the crack-tip and again a part of the stress energy is absorbed.

The role of the grain size itself on the value of the fracture toughness and fracture energy is not quite clear in the literature. For cubic materials Rice *et al.* [15] do not expect that the grain size affects the fracture energy (and fracture toughness) considerably. Veldkamp and Hattu [16] found a decrease of K_{Ic} for cubic nickel–zinc ferrite from 1.6 MPa $m^{1/2}$ at a grain size of 2 μm to 1.0 MPa $m^{1/2}$ at a grain size of 35 μm. They also reported that K_{Ic} for hexagonal Al_2O_3 is independent of the grain size contrary to what is expected for non-isotropic materials [17, 18]. Simpson [17] reports a remarkable decrease of the fracture energy with increasing grain size for alumina while Monroe and Smyth [18] found a small increase of the fracture energy with increasing grain size; both cases refer to dense materials.

Pratt [19] suggests that differences in grain boundary behaviour and a change in the fracture mechanism as a function of the grain size may be the cause of the different results of some authors. Also the measurement technique may play an important role. According to Pratt bend test methods with small notches compared with the width of the samples, sharp cracks and fast cross-head speeds gave the best results. Impurities and impurity segregation can also affect the bonding of the grains and can change the fracture mechanism from transgranular to intergranular with decreasing grain size. Examining various fracture energy data in the literature, it is found that these energy values tend to increase with decreasing grain size provided the crack growth is sufficiently rapid [19].

In this investigation sintering experiments with pure yttria-stabilized zirconias are carried out to obtain samples with different grain sizes and equal, low porosity values. The fracture energy is measured as a function of the grain size and the type of fracture is determined.

In a second series of experiments an amount of Bi_2O_3 is added to the pure zirconia powder. The main purpose of this addition was to lower the sintering temperature [2, 6] and to modify the grain boundary properties. The result of this procedure is a microstructure of a cubic main phase in which a certain amount of a monoclinic ZrO_2 phase is present. The effect of the monoclinic phase and the addition of Bi_2O_3 on the fracture energy and the type of fracture is measured. For the fracture toughness measurements the results of 3- and 4-point bend tests are compared with the results obtained by the indentation technique.

2. Experimental procedure

Pure single-phased yttria-stabilized zirconia ceramics with an average grain size of 2 μm or more and a relative density of at least 95% was prepared using a fine grained powder. This zirconia powder was commercially available by Zircar Products Inc., type ZYP stabilized with 12 wt% yttria.

Samples (Z1, Z2 and Z3) were isostatically pressed at 400 MPa and sintered at temperatures given in Table I. In order to produce a pure stabilized zirconia ceramic with a grain size less than 1 μm and high density, it was necessary to use the alkoxide method described by van de Graaf *et al.* [8]. This resulted in an ultrafine grained powder which was sintered without bismuthoxide or other sinter aids to densities of 98% at temperatures less than 1500 K (Table I, sample A1). The difference in starting powder (zircar or alkoxide) did not effect the mechanical properties or fracture behaviour of the material (see Section 3.2.1).

In the samples Z4 and Z5 Bi_2O_3 was introduced to the zircar powder by means of dry milling. For the samples of the S-series the raw materials ZrO_2, Y_2O_3 and Bi_2O_3 with grain sizes of about 10 μm were thoroughly mixed and calcined at about 1350 K. After grinding in isopropanol for three hours the powders were isostatically pressed at about 400 MPa and reactively sintered at temperatures given in Table I.

A Philips X-ray diffractometer PW 1370 with Cu$K\alpha$-radiation was used to identify the present crystal phases and the lattice parameter of the main phase was calculated using silicon or $Pb(NO_3)_2$ as internal standards.

The ceramic microstructures were investigated on polished and thermal etched samples and on fracture surfaces of samples with the scanning electron microscope JEOL JSM U3. The average grain size was determined with the line intercept method

TABLE I The microstructure, phases and impurities of various ZrO_2–Y_2O_3–Bi_2O_3 samples

Sample number*	Sintering temperature (K)	Density† (g cm^{-3} (%))	Average grain size (μm)	Phases‡	Impurities (wt %)		Sample compositions (mol %)		
					SiO_2	Al_2O_3	(ZrO_2 + HfO_2)	Y_2O_3	Bi_2O_3
Z1	1973	5.76(97)	50	F	0.05	0.04	92.5	7.5	–
Z2	1773	5.70(96)	13	F (0.5135)	0.05	0.04	92.5	7.5	–
Z3	1626	5.64(95)	2.6	F	0.05	0.04	92.5	7.5	–
A1	1493	5.82(98)	0.7	F (0.5141)	0.04	0.03	91.1	8.9	–
Z4	1208	5.64(93)	0.6	F (0.5161) + M (31)	0.05	0.04	90.3	7.4	2.3
Z5	1329	5.70(95)	0.65	F (0.5155) + M (20)	0.05	0.04	91.1	7.45	0.85
S8b	1420	5.73(94)	5.0	F (0.5152) + M (15) + U	0.62	0.10	88.8	8.9	2.3
S9b	1420	5.75(94)	3.8	F (0.5155) + M (10) + U	0.14	0.08	88.0	8.7	3.3
S12	1570	5.75(95)	20	F (0.5146)	0.14	0.08	90.2	8.9	0.9
S8a	1420	5.78(95)	–	F (0.5157) + M (11) + U	0.62	0.10	88.8	8.9	2.3
S9a	1420	5.78(95)	–	F (0.5158) + M (11) + U	0.14	0.08	88.0	8.7	3.3

*For S, Z and A samples see Preparation (Z is Zircar products Inc., Florida, New York, USA).

†Figures in parenthesis are percentage densities of the theoretical density.

‡F is the fluorite phase with the lattice parameter, a, in nm given in parentheses; the standard deviation is better than 0.0002 for all samples, M is monoclinic phase with the amount present in wt % given in parenthesis, U is an unidentified phase.

using corrections according to the method of Mendelsohn [20].

X-ray fluorescence spectrometry was carried out with a Philips PW 1410 spectrometer to determine the overall composition of the samples [21]. Silica and alumina impurities were determined by the method reported by Kruidhof [22].

The Young's modulus E and Poisson's ratio ν were measured at 10 and 20 MHz by a pulse-echo method [23]. The fracture toughness, K_{Ic}, was measured using the three-point bend test at a crosshead speed of $5\,\mu m\,sec^{-1}$ and with a sample dimension of 1 by 3 by 15 mm. The notch width was $50 \pm 5\,\mu m$ and precracking techniques were not applied. For sample S8a and S9a the indentation technique as described by Evans and Charles [24] was used to determine the fracture toughness (K_c) value. The sample surface was polished and annealed at 1073 K and loads of 100 to 400 N were applied. These indentation measurements were compared with bending tests. From these measurements we may conclude that for accurate fracture toughness values a bending test is recommended (see Appendix).

3. Results and discussion

3.1. Materials characteristics

Various data on the samples are summarized in Table I. The sample densities are all between 93 and 98%.

Single-phased yttria-stabilized zirconia ceramics with grain sizes between 0.7 and 50 μm have been prepared. The small difference in chemical composition of the Bi_2O_3 free samples (see Table I) was introduced for electrical purposes [10]. For mechanical properties this difference is not important. All these materials have a cubic fluorite structure.

For bismuth containing samples a dense material can be obtained at temperatures as low as 1208 K.

By means of substitution with 0.8 to 3.5 mol % Bi_2O_3, in these materials a certain amount of a monoclinic ZrO_2-rich phase appears. The amount of this monoclinic phase depends on the sintering temperature, the raw material morphology and the Y/Zr-ratio in the material. More monoclinic second phase appears at lower sintering temperatures and at lower Y/Zr-ratio [2, 6]. At temperatures between 1300 and 1500 K the composition of the main fluorite phase tends to be constant at the composition 0.86 ZrO_2–0.13 Y_2O_3–0.01 Bi_2O_3 [2, 25]. Except for sample S8 all samples have a low impurity level.

3.2. Mechanical properties

3.2.1. Pure yttria-stabilized zirconia

The fracture toughness values measured by means of bending tests are given in Table II. For pure yttria-stabilized zirconia K_{Ic} decreases from 4.1 to 1.8 MPa $m^{1/2}$ with an increase of the grain size from 0.7 to 50 μm. Ingel *et al.* [26] found a fracture toughness value $\leqslant 1.7$ MPa $m^{1/2}$ for a single crystal containing 20 wt % Y_2O_3.

The fracture energy γ (J m^{-2}) can be calculated now using Equation 1 provided that values for E and ν are known [17]:

$$\gamma = \frac{(1-\nu^2)K_{Ic}^2}{2E}. \quad (1)$$

Values for ν and E were measured independently and are first discussed.

Poisson's ratios ν of 0.30 to 0.31 are found. Its value increases slightly with decreasing porosity.

In Table II values of Young's modulus (E) are given for several samples. The Young's modulus is grain-size independent but depends on the porosity. The experimental results can be fitted according to the relation:

$$E(\text{GPa}) = (221 \pm 4)\exp[(-2.7 \pm 0.5)P] \quad (2)$$

where P is the porosity. The correlation coefficient for this relation is 97.5% and the deviation is given in the 90% reliability interval. The values for E calculated with Equation 2 are in good agreement with the values given by Lange [27, 28] for tetragonal, dense ZrO_2 (207 GPa) and for a material with 10% porosity (165 GPa). The Young's modulus of a single crystal of yttria-stabilized zirconia (210 GPa [26]) also agrees rather well with a ceramic sample with zero porosity (see Equation 2).

The E-values according to Equation 2 are much

TABLE II Fracture toughness (K_{Ic}) and Young's modulus (E) values for various samples

Sample number	K_{Ic}* (MPa $m^{1/2}$)	E (GPa)
Z1	1.84(7)	204
Z2	2.11(12)	198
Z3	2.84(3)	192
A1	4.12(16)	210
Z4	1.84(7)	
Z5	2.09(14)	
S8b	1.81(6)	188
S9b	1.78(8)	185
S12	1.97(5)	

*The standard deviation of the last decimal figure is given in parentheses.

higher than those mentioned by Rice *et al.* [15] and Gupta *et al.* [1]. Rice *et al.* give a value of 145 GPa for an yttria-stabilized zirconia (ZrO_2–12 wt% Y_2O_3) with 1% porosity and 97 GPa for the same material with 10% porosity. The Young's modulus given by Rice is independent on the grain size (0.4 to 5 μm) and the composition of the materials.

Gupta *et al.* [1] found the same value of 145 GPa for the Young's modulus of partially stabilized zirconia but no porosity values are given. Finally relatively low, apparent elastic moduli are caused by (micro)crack systems, which are not improbable for Gupta's materials because of the existence of a second phase.

A problem, however, is that these authors [1, 15] do not report the way they measured E. Now it is well known that E-values measured acoustically are considerably higher than those measured mechanically. This probably can explain the observed differences.

According to Equation 1 the fracture energy of these dense materials are calculated now. The experimental results can be fitted according to the relation:

$$\gamma\,(\mathrm{J\,m^{-2}}) = (3 \pm 2) + (27 \pm 3)d^{-1/2} \quad (d \text{ in } \mu\mathrm{m}) \qquad (3)$$

with a correlation coefficient of 99.8% and the deviation is given in the 90% reliability interval. This result is plotted in Fig. 1 which shows that the fracture energy increases with decreasing grain size.

The pure stabilized zirconia has a transgranular fracture behaviour for every grain size mentioned in Table I. This is shown in Fig. 2a for sample Z2. In most cases an intergranular fractured surface is found in the literature for materials with such small grains [14]. The different fracture behaviour in our materials may be due to strong grain boundaries and/or a certain orientation between the grains in such a way that the cleavage planes with the lowest binding energies are almost normal to the greatest principal applied stress [19]. The latter situation is not very possible in ceramics.

The strong effect of the average grain size on the fracture energy of this material is somewhat unexpected because it has a cubic symmetry. According to Rice *et al.* [15] isotropic materials should have a grain size-independent fracture energy. A point of discussion is the interpretation of the fracture energy results of Rice *et al.* [15]

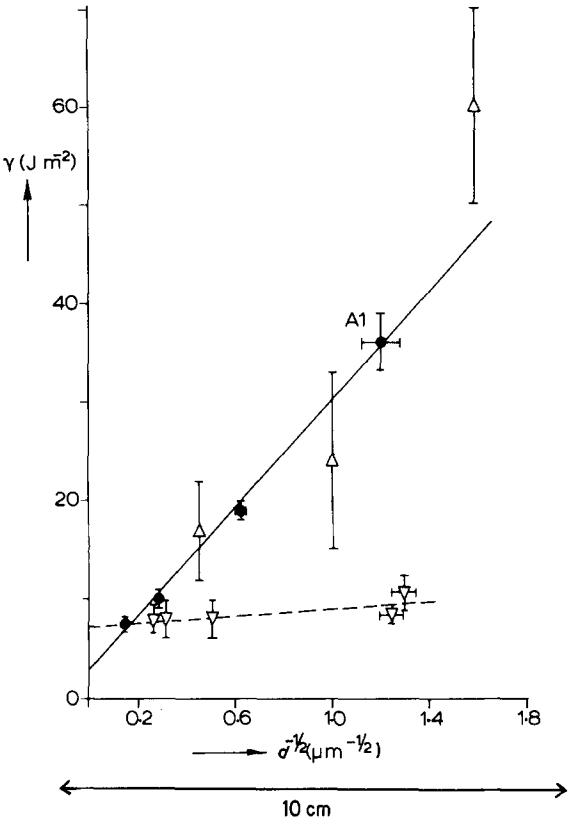

Figure 1 The fracture energy γ (J m^{-2}) of stabilized zirconias as a function of the inverse square root of the average grain size d (• Bi_2O_3-free samples; ▽ Bi_2O_3-containing samples; △ Data of Rice *et al.* [15] for zirconia samples with 6, 8 and 12 wt% Y_2O_3).

and Lange [27, 28] as a function of the composition and grain size. To obtain the same porosity for each composition it is necessary to change the sintering temperature and therefore most likely the grain size will be different. The amount of tetragonal and cubic phase also changes and most authors interprete their results exclusively in terms of the amount of tetragaonal phase. In our opinion the effect of the grain size itself is overlooked but is also important especially if a transgranular fracture occurs. This point will be discussed below. The number of grain boundaries that the crack has to pass increases considerably with decreasing grain size. If the fracture energy is dominated by the energy necessary for crack initiation at the grain boundaries this should explain qualitatively the observed experimental results. This is supported by the fact that the shape of Equation 3 is equal to that of the well-known Petch (or Orowan) equation, which relates

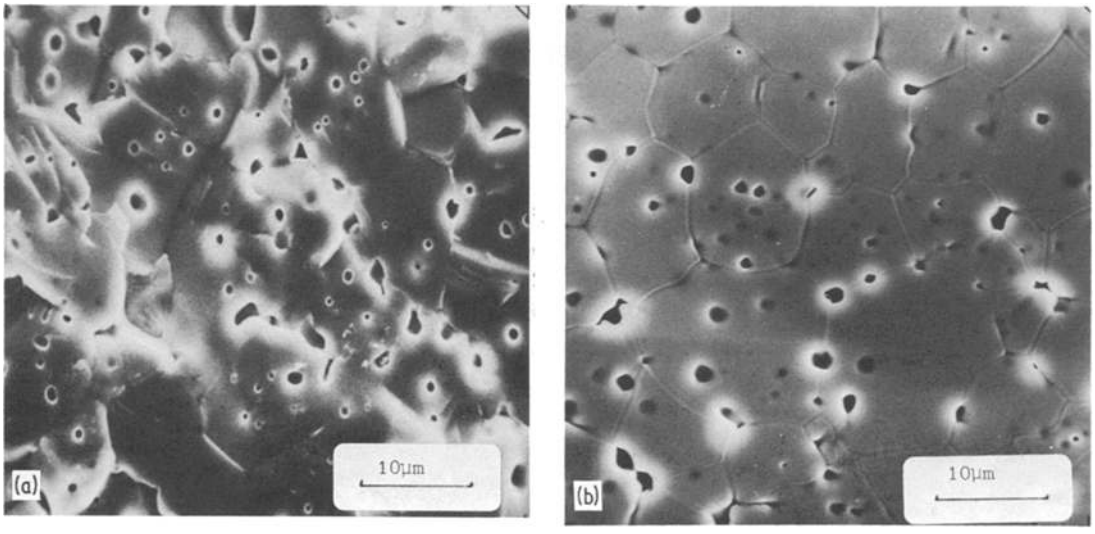

Figure 2 (a) A fracture surface of a ZrO_2–Y_2O_3 sample (Z2). (b) A polished and thermal etched surface of sample Z2.

the mean strength of a sample to the mean grain size. This equation suggests an energy-absorbing stress release mechanism on the grain boundaries. Carniglia [29] found that experimental data could be fitted with this equation especially the data for cubic MgO and $MaAl_2O_4$ materials.

The fracture energy results presented by Rice *et al.* [15] for the samples ZrO_2 with 6, 8 and 12 wt% Y_2O_3 and grain sizes of 0.4, 1.0 and 5.0 μm are compared with ours and fitted in Fig. 1. It can be seen that the fit to a linear relationship of γ (J m^{-2}) with $d^{-1/2}$ (μm$^{-1/2}$) is not very good but there is undoubtedly an increase of the fracture energy with decreasing grain size. The values of the fracture energy Rice *et al.* [15] found, are about the same we found for ZrO_2 with 14 and 16 wt% Y_2O_3 at about the same grain sizes (see Fig. 1). This indicates that the results of Rice *et al.* can at least be partially interpreted in terms of grain size effects instead of completely by the effect of phase transformations.

Gupta *et al.* [1] found fracture energy values of 100 to 200 J m^{-2} for samples with 2 to 3 wt% Y_2O_3 and grain sizes of 0.3 μm. At this grain size we calculate with Equation 3 a fracture energy value of 55 J m^{-2} for our materials. So in this case the stress-induced phase transition plays the most important role for the toughening of the material contrary to the above mentioned case of Rice *et al.* [15].

3.2.2. Bi_2O_3 doped material

The K_{Ic}-values for Bi_2O_3-containing and Bi_2O_3-free samples show a different behaviour. The K_{Ic}-values of the Bi_2O_3 samples are between 1.78 and 2.09 MPa m$^{1/2}$ and there is not or only a slight dependence on the grain size. The fracture energy is also almost independent of the grain size (9 ± 3 J m^{-2}) (see Fig. 1).

The fracture behaviour of the two types of materials differs strongly. Bi_2O_3-containing materials have an intergranular fracture behaviour even at low Bi_2O_3-contents (0.5 mol% Bi_2O_3). This is illustrated in Fig. 3a for a material with about 1 mol% Bi_2O_3 sintered at 1373 K. A polished and thermal etched surface is shown in Fig. 3b where the monoclinic phase can be found on the grain boundaries of the main phase. These smaller grains are not found in the Bi_2O_3 free materials (see Fig. 2b).

The monoclinic phase of micron and submicron size weakens the bonding of the grains through which the intergranular fracture proceed. The length of a crack through a material is for intergranular cracks about two times larger than for transgranular cracks, independent of the grain size. This grain size independency of the crack length may explain the effect that the energy for intergranular fracture in these materials is independent of the grain size.

The monoclinic ZrO_2 phase can enhance K_{Ic} according to literature [13, 14]. The fact that we do not find such a result is probably due to the rather unfavourable distribution of the second phase which is situated exclusively along grain boundaries of the main phase in rather small

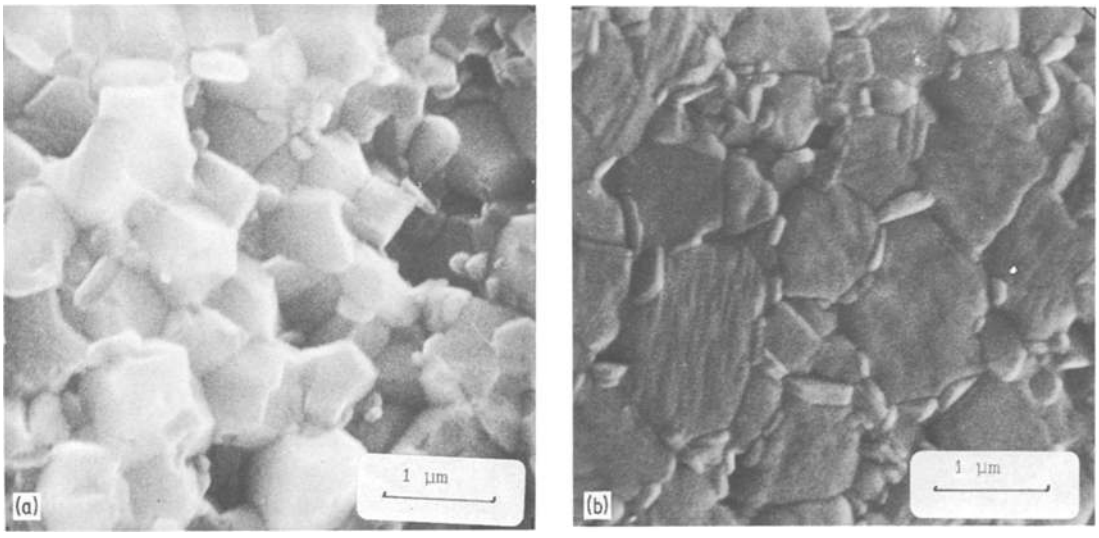

Figure 3 (a) A fracture surface of a ZrO_2–Y_2O_3–Bi_2O_3 sample with 1 mol% Bi_2O_3 sintered at 1373 K. (b) A polished and thermal etched surface of a ZrO_2–Y_2O_3–Bi_2O_3 sample with 2 mol% Bi_2O_3 sintered at 1293 K.

particles [25]. This morphology does not fulfill the requirements for enhancing K_{Ic} [13, 14].

4. Conclusions

The fracture energy of pure, single-phased ZrO_2–Y_2O_3 ceramics with fluorite structure increases with decreasing grain size. A linear relation between the fracture energy and the inverse square root of the average grain size has been found. All these materials show a transgranular fractured surface.

Young's modulus and Poisson's ratio have been measured separately. Young's modulus values of 185 to 220 GPa are obtained at porosities of 7 to 0.5%, respectively.

It is made probable that grain size effects play also a role in the increase of the fracture toughness and fracture energy of partially stabilized materials with a tetragonal phase.

Most Bi_2O_3-containing samples consist of two phases, a fluorite phase and a monoclinic phase consisting mainly of zirconia and a small amount of Bi_2O_3. After fracture these samples exhibit an intergranular fractured surface. The fracture energy of the Bi_2O_3-containing samples is independent of the grain size at a value of $9 \pm 3\ J\ m^{-2}$.

The fracture toughness has been measured by the indentation method and by the bend test and the results have been compared. The simple indentation method can be useful to estimate the fracture toughness but for accurate measurements other test methods (e.g. the bend test) are necessary.

Acknowledgement

The authors are indebted to Dr G. de With of Philips Research Laboratories for performing Young's modulus measurements.

Appendix: Comparison of the bend test method and the indentation technique

For the determination of fracture toughness values several types of test methods are in use. A simple and economic test procedure is the Vickers indentation technique [1, 24, 30]. Evans and Charles [24] evaluated this indentation technique by comparing the fracture toughness of various materials, determined by the double-torsion technique, with data obtained by the Vickers indenter. For theoretical considerations and calibration they obtained a graph with

$$\frac{K_c\Phi}{H(a)^{1/2}}\left(\frac{H}{\Phi E}\right)^{0.4} \text{ against } c/a \qquad \text{(A1)}$$

where Φ is the constraint factor (≈ 3), H is the hardness (GPa), a is the impression radius and c is the crack length as given by [24].

With this graph K_c-values have been calculated for two samples measured with the indentation technique at 4 different loads (Table AI). Anstis *et al.* [30] also evaluated the indentation technique. They took into account that after unloading the radial cracks grow further to their final

TABLE AI Comparison of the indentation technique at different loads with the bend test method for the determination of fracture toughness K_c

Measuring method	Sample number			
	S8a		S9a	
	K_c (MPa m$^{1/2}$)		K_c (MPa m$^{1/2}$)	
	Equation A1	Equation A2	Equation A1	Equation A2
Indenter load 100N			3.5	3.6
Load 200N	4.7	4.7	4.1	3.5
Load 300N	2.1	1.7		
Load 400N			2.4	2.0
4-point bend test according to Claussen [31]	2.2*(1)			
3-point bend test according to de With [32]	2.21(7)		1.57(4)	

*Standard deviation of the last decimal figure is given in parentheses.

length as a consequence of residual stresses and they obtained

$$K_c = \S (E/H)^{1/2} (P/C_0^{3/2}) \qquad \text{(A2)}$$

where § is a material-independent constant for Vickers-produced radial cracks, P is the peak load and $C_0 = c$, the crack length appropriate to the post indentation equilibrium configuration. The "calibration" constant § $= 0.016 \pm 0.004$ and is obtained by Anstis *et al.* [30] by averaging over the data of K_c-values measured with double torsion and double-cantilever beam techniques.

With Equation A2 K_c-values were calculated for samples S8a and S9a at 4 different loads (Table AI). The K_c-values of these samples were also obtained with the 4-point and 3-point bend test. From Table AI it can be seen that the results, calculated with Equations A1 and A2, are in good agreement within the commonly achieved accuracy of 10 to 25% of these methods. With increasing load the calculated K_c-values, obtained with the indentation technique, are comparable with the bend test methods for sample S8a. The K_{Ic}-values measured with the 4-point and 3-point bend test method are in excellent agreement.

From this result it can be concluded that one has to be very careful with the interpretation of K_c-values obtained by the indentation technique. The grain size, surface roughness and surface stresses can affect the crack dimensions considerably. After comparison with other measuring methods and after eliminating load effects this extreme fast and simple method can be used to obtain an estimate of the K_c-value, especially for large series of samples. However, the determination of more accurate fracture toughness values required other test methods.

References

1. T. K. GUPTA, F. F. LANGE and H. BECHTOLD, *J. Mater. Sci.* 13 (1978) 1464.
2. K. KEIZER, A. J. BURGGRAAF and G. DE WITH, *ibid.* 17 (1982) 1095.
3. K. C. BRADFORD and R. J. BRATTON, *ibid.* 14 (1979) 59.
4. J. F. SCHACKELFORD, P. S. NICHOLSON and W. N. SCHMELTZER, *Amer. Ceram. Soc. Bull.* 53 (1974) 86.
5. H. TAKAGI, S. KAWABARA and H. MATSOMOTO, *Sprechsaal* 107 (1974) 584.
6. K. KEIZER, M. J. VERKERK and A. J. BURGGRAAF, *Ceramurgia Int.* 5 (1979) 143.
7. K. S. MAZDIYASNI, C. T. LYNCH and J. M. SMITH II, *J. Amer. Ceram. Soc.* 50 (1967) 532.
8. M. A. C. G. VAN DER GRAAF, K. KEIZER and A. J. BURGGRAAF, "Science of Ceramics" Vol. 10, edited by H. Hausner (DKG Weiden, 1980) p. 83.
9. M. HOCH and K. M. NAIR, *Ceramurgia Int.* 2 (1976) 80.
10. M. J. VERKERK, B. J. MIDDELHUIS and A. J. BURGGRAAF, *Solid State Ionics* 6 (1982) 159.
11. R. C. GARVIE, R. H. J. HANNINK and R. T. PASCOE, *Nature* 258 (1975) 703.
12. T. K. GUPTA, R. B. GREKILA and E. C. SUBBARAO, *J. Electrochem. Soc.* 128 (1981) 929.
13. N. CLAUSSEN, J. STEELE and R. F. PABST, *Amer. Ceram. Soc. Bull.* 56 (1977) 559.

14. N. CLAUSSEN and J. JAHN, *Ber. Dt. Keram. Ges.* **55** (1978) 487.
15. R. W. RICE, R. C. POHANKA and W. J. McDONOUGH, *J. Amer. Ceram. Soc.* **63** (1980) 703.
16. J. D. B. VELDKAMP and N. HATTU, *Phil. J. Res.* **34** (1979) 1.
17. L. A. SIMPSON, *J. Amer. Ceram. Soc.* **56** (1973) 7.
18. L. D. MONROE and J. R. SMYTH, *ibid.* **61** (1978) 538.
19. P. L. PRATT, *Met. Sci.* **14** (1980) 363.
20. M. I. MENDELSOHN, *J. Amer. Ceram. Soc.* **52** (1969) 443.
21. J. H. G. VAN WILLIGEN, H. KRUIDHOF and E. A. M. F. DAHMEN, *Anal. Chim. Acta* **62** (1972) 279.
22. H. KRUIDHOF, *Anal. Chim. Acta* **99** (1978) 193.
23. H. F. POLLARD, "Sound Waves in Solids" (Pion Ltd., London, 1977).
24. A. G. EVANS and E. A. CHARLES, *J. Amer. Ceram. Soc.* **59** (1976) 371.
25. A. J. A. WINNUBST, M. J. VERKERK and A. J. BURGGRAAF, Advanced Ceramics 5 (1982) to be published.
26. R. P. INGEL, R. W. RICE and D. LEWIS, *J. Amer. Ceram. Soc.* **65** (1982) C108.
27. F. F. LANGE, *J. Mater. Sci.* **17** (1982) 240.
28. *Idem, ibid.* **17** (1982) 255.
29. S. C. CARNIGLIA, *J. Amer. Ceram. Soc.* **55** (1972) 234.
30. G. R. ANSTIS, P. CHANTIKUL, B. R. LAWN and D. B. MARSHALL, *ibid.* **64** (1981) 533.
31. N. CLAUSSEN, private communication (1981).
32. G. DE WITH, private communication (1982).

Received 21 May
and accepted 29 November 1982